New 224 nm Hollow Cathode Laser–UV Raman Spectrometer

MARK C. SPARROW, JOHN F. JACKOVITZ, CALUM H. MUNRO, WILLIAM F. HUG, and SANFORD A. ASHER*

Department of Chemistry, University of Pittsburgh, Pittsburgh, Pennsylvania 15260 (M.C.S., S.A.A.); Bechtel Bettis Inc., P.O. Box 79, West Mifflin, Pennsylvania 15122 (J.F.J.); PPG Industries, Research Center, 4325 Rosanna Dr., Allison Park, Pennsylvania 15101 (C.H.M.); and Photon Systems, 712 Arrow Grand Circle, Covina, California 91722 (W.F.H.)

We have developed an optimized high-throughput UV Raman spectrometer that utilizes a simple, inexpensive new 224.3 nm hollow cathode laser. This quasi-continuous wave (CW) 224.3 nm laser can be used to detect sub-ppm concentrations of aromatic and polycyclic aromatic hydrocarbons in aqueous solutions. This excitation is also useful for studying aromatic amino acids in proteins. We demonstrate the utility of this spectrometer to study the environments of tyr and trp in horse heart myoglobin.

Index Headings: **Raman spectroscopy; Instrumentation; Lasers; Proteins.**

INTRODUCTION

UV resonance Raman spectroscopy (UVRS) is a powerful tool to examine molecular structure and dynamics.[1,2] The high UVRS signal-to-noise ratios make it possible to study trace analytes such as polycyclic aromatic hydrocarbons[1–3] and to study dilute protein and peptide solutions.[4,5] Its high spectral selectivity makes it ideal for the study of aromatic amino acid environments in proteins.[6] We recently demonstrated that UVRS excited within the $\pi \rightarrow \pi^*$ amide peptide absorption bands is the most powerful dilute solution methodology to determine protein secondary structure.[4] It clearly is the most powerful methodology available for the study of the first steps in protein folding and unfolding.[7]

Although UVRS is a powerful spectroscopic technique, it has found rather slow acceptance due to the cost and complexity of previous laser sources[2,8,9] and the fact that UVR spectrometers have not been commercially available. Over the last decade, up until 1998, we evaluated a number of commercial Raman spectrometers that claimed to operate in the UV at $\lambda < 250$ nm. None of these instruments had adequate performance.

The first UV laser sources were low-repetition-rate nanosecond YAG lasers, which were frequency doubled to pump dye lasers, which were then frequency doubled and mixed to obtain tunable UV excitation.[10] Alternative strategies utilized frequency-tripled and -quadrupled YAG lasers followed by Raman shifting.[2,11] The duty cycle of these lasers was very small (10^{-8}). This condition resulted in high pulse energies and high incident fluences, which resulted in nonlinear optical phenomena, making Raman spectral measurements more complicated.[12,13] The use of frequency-doubled, high-repetition-rate excimer laser-pumped dye lasers increased the duty cycle 100-fold, but nonlinear phenomena could still pose spectral measurement challenges.[13] The development of the intracavity frequency-doubled Ar^{++} and Kr^{+++} lasers solved these problems since the lasers were continuous wave (CW).[8,9] These lasers are quite reliable, but are expensive.

In the work here, we describe a new 224.3 nm optimized UVR spectrometer that utilizes a new, relatively inexpensive laser. This hollow cathode laser is small, has a relatively high electrical power efficiency, and requires no water cooling. We believe that this laser source presents revolutionary opportunities to develop portable, inexpensive UVR spectrometers.

EXPERIMENTAL

Acetonitrile and sodium perchlorate were purchased from Fisher Scientific. Horse heart myoglobin (Mb) was purchased from Sigma. Dodecyldimethylamine was purchased from Akzo-Nobel, and the benzoic acid (BA) was purchased from Alrich. The Raman cross sections of tyr and trp were calculated from previously determined values of the absolute Raman cross sections of the 932 cm^{-1} band of perchlorate and the 918 cm^{-1} band of acetonitrile.[14]

The Mb samples were circulated through the beam as a temperature-controlled, free surface flow stream.[7] The use of a free surface avoids sample decomposition on window surfaces and interference from the broad silica Raman bands. Raman scattering was collected by a pair of plano-convex silica lenses and dispersed by the Raman spectrometer described below.

The dodecyldimethylamine and benzoic acid solutions were measured with a micro Raman spectrometer similar to that reported previously,[15] where an Olympus B×60 microscope was coupled to a Spex 1702 monochromator. Light was collected with a 36× Cassegrain objective, and the sample was illuminated by reflection of focused laser light by a small prism attached to the center of the objective.

RESULTS AND DISCUSSION

Hollow Cathode HeAg Laser. Figure 1 illustrates the design of the HeAg 224.3 nm hollow cathode laser tube. The active medium of this laser is singly ionized silver ions formed by sputtering within a silver hollow cathode tube with a 3 mm inside diameter and a 40 cm length. Helium and other dopant gases are employed as buffer gases to ionize and excite sputtered silver atoms in a charge transfer pumping reaction: $2He^+ + Ag \rightarrow (Ag^{++})^* + 2He$. Lasing involves the $4d^95d^1 \rightarrow 4d^95p^1$ transition.[16]

The hollow cathode discharge is formed between the hollow cylindrical silver cathode and a transverse anode

Received 15 June 2000; accepted 30 August 2000.
* Author to whom correspondence should be sent.

0003-7028/01/5501-0066$2.00/0

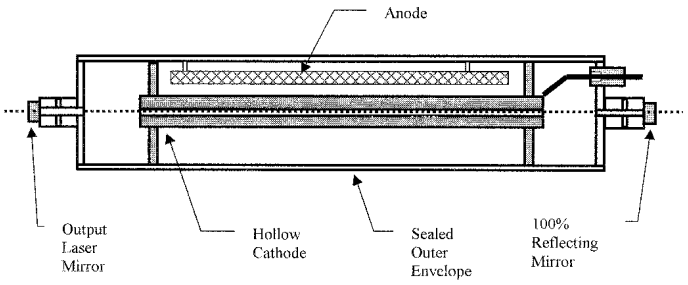

FIG. 1. Hollow cathode laser tube.

via a slot in the side of the cathode. The buffer gas pressure mixture is optimized for output at 224.3 nm. The threshold discharge current for laser output is less than 1 A, and the optimum output is achieved at a current ~ 12 A. The voltage drop is about 350 V.

The 224.3 nm laser transition is a CW transition with a demonstrated output of >120 mW at 224.3 nm with the use of the 40 cm cathode, a flat 0.75% transmission output-coupling mirror, and a 2 m concave high reflecting mirror. Output is achieved within 15 ms after application of voltage between the anode and cathode. The output remains constant as long as the voltage is applied. After termination of the voltage, the laser output decays with an exponential time constant of ~ 10 ms.

The laser output beam diameter is ~ 2.5 mm with a divergence of ~ 0.3 mR. The emission linewidth is less than 3 GHz (0.1 cm^{-1}), and the line position is fixed. The longitudinal mode spacing is 257 MHz. The transverse mode of the laser is multimode with a "times diffraction limit" of about 18.

The laser output is insensitive to ambient temperature and requires no warm-up or other preheating and no temperature regulation. The laser head and power supply are designed for operation at an average input power of <100 W in order to keep the system air cooled and simple. In order to provide the discharge conditions needed for optimum output (12 A at 350 V = 4.2 kW) and to keep the average input power below about 100 W, the input power is switched with a maximum, long-term duty cycle of <3%. The average output power is therefore restricted in the present design to less than ~ 3 mW at 224.3 nm.

The mode quality of the output beam was determined from the measured, focused spot size, and gave a value of $m^2 = 18$. This approach allows us to calculate the focused spot size on the sample, d:

$$d = \frac{4m^2\lambda f}{\pi D} \quad (1)$$

where f is the focal length of the focusing lens, D is the beam diameter (2.5 mm), and λ is the laser wavelength (224.3 nm). Therefore these lasers can be focused to a ~ 5 μm spot with a 2.5 mm focal length, 0.5 NA (numerical aperture) microscope objective.

Figure 2 shows the Raman spectrometer. The laser light is simultaneously steered and frequency-filtered by a pair of Pellin–Broca prisms. This arrangement is especially necessary for the HeAg laser due to its intense, nonlasing plasma lines. These prisms also separate the frequency-doubled output from the fundamental output of the Ar^{++} laser.

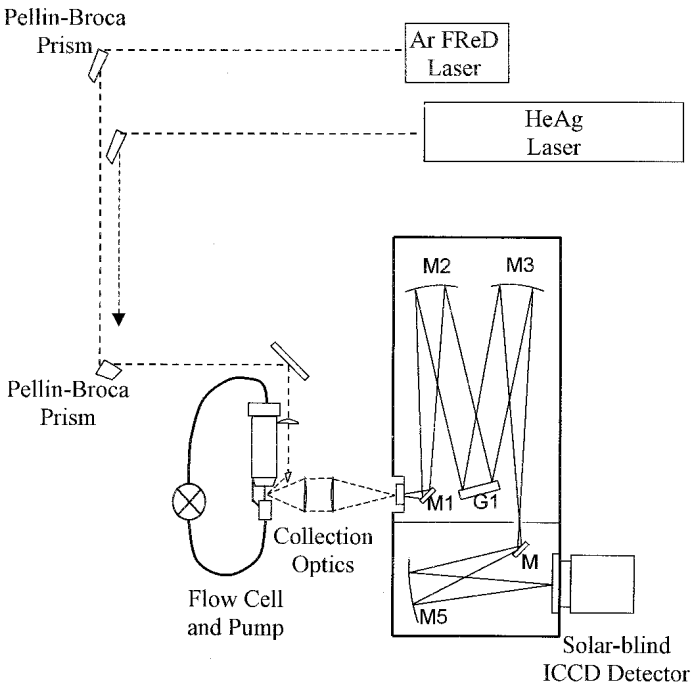

FIG. 2. Schematic diagram of the Raman spectrometer. The HeAg laser provides 224.3 nm excitation. The frequency-doubled Ar^+ laser provides 228.9, 238,2, and 244 nm excitation wavelengths. Pellin–Broca prisms are used for beam steering and elimination of plasma lines.

Figure 2 also shows the Czerny–Turner spectrograph ($f/\# = 7$), which uses a second stage to reimage the dispersed light in order to reduce the stray light on the charge-coupled device (CCD) detector. The mirrors were dielectrically coated (CVI Laser, Inc.) to have a 40% reflectivity at 224.3 nm and >95% reflectivity for light at 229.4 nm (a 1000 cm^{-1} Raman shift). These five mirrors and the grating (50% efficiency) are expected to give throughputs of ~ 0.5% at 224.3 nm and ~ 39% at 229.4 nm.

We used a solar-blind intensified CCD detector made by Roper Scientific (IMAX-1024 × 256). This solar-blind intensifier has a very low equivalent background illumination, which improves the spectral signal-to-noise ratios (SNRs). In addition, we tested numerous CCD detectors (backthinned as well as coated with fluorophores) and found that the intensified CCD gave much higher SNRs. This occurred even when the technical specifications indicated that the unintensified detectors should give better SNRs. We did not completely characterize the origin of the poor SNRs from these other detectors. The major factor appeared to be a low sensitivity to UV light, since these detectors operated well in the visible spectral region. The detector specification normally indicates photocathode responsivity. However, actual measurements of spectral SNRs have this parameter convoluted with the intensifier gain, the intensifier equivalent background illumination, and the number of CCD-detected events per photon counted and the detector readout noise. Our conclusions about the utility of the other detectors result from experiments which exchanged different detectors on one spectrometer that was illuminated by a low-intensity UV source.

The 228.9, 238.2, and 244 nm doubled Ar^+ laser lines of s- and p-polarizations and the 224.3 nm HeAg laser

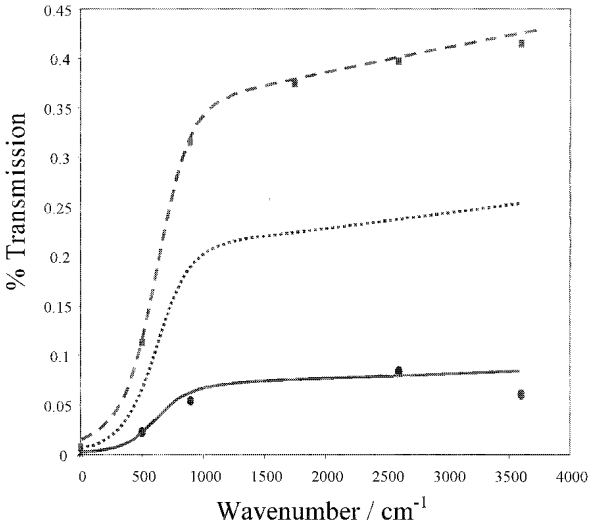

FIG. 3. Calculated efficiencies of the monochromator for 224.3 nm Raman excitation. The efficiency curve for randomly polarized light was used for correcting spectra acquired with the HeAg laser. (●) Measured values (*s*-polarization), (■) measured values (*p*-polarization), (———) calculated efficiency (*s*-polarization), (·····) calculated efficiency (random polarization), (– – –) calculated efficiency (*p*-polarization).

line were used to measure the spectrograph throughput efficiency. The ~1 mW laser beams were directed through the spectrograph entrance slit, and the transmitted power was measured at the detector image plane. The values for *s*- and *p*-polarized light are shown in Fig. 3. The effective monochromator efficiency is the average of that for *s*- and *p*-polarizations. We empirically found that the expression

$$T(\nu) = A * \frac{e^{N\nu + M}}{e^{N\nu + M} + B} + (D\nu + C) \qquad (2)$$

accurately models throughput at 224.3, 228.9, 238.2, and 244 nm. $T(\nu)$ is the percent transmission of the monochromator at the Raman shifted frequency (cm^{-1}), where $A = 0.3213$, $B = 61.3024$, $C = 0.007251$, $D = 0.00002613$, $N = 0.007471$, and $M = -0.5264$ are fitting constants for *p*-polarization. The fit constants for *s*-polarization are $A = -9.6841$, $B = 12\,692.3261$, $C = 9.8035$, $D = -0.0008987$, $N = -0.004572$, and $M = -12.7368$. The measured 224.3 nm Raman spectra were spectrometer-efficiency corrected by using the relationship

$$I_{corr}(\nu) = \frac{I_o(\nu)}{T(\nu)} \qquad (3)$$

where $I_{corr}(\nu)$ is the corrected intensity, $I_o(\nu)$ is the observed intensity, and $T(\nu)$ is the calculated frequency-dependent throughput of the monochromator.

Figure 4 illustrates the performance of the spectrometer for neat acetonitrile in a quartz cell, a calcite crystal, and a block of Teflon®. Raman bands as close as 200 cm^{-1} from the Rayleigh line are easily observed for nonturbid samples. The spectrum of calcite shows the strong Raman band at 280 cm^{-1}. The spectrum of Teflon® shows that, although highly scattering samples show significant Rayleigh scattering at low frequencies, Raman spectra can be easily measured down to less than 400 cm^{-1} from

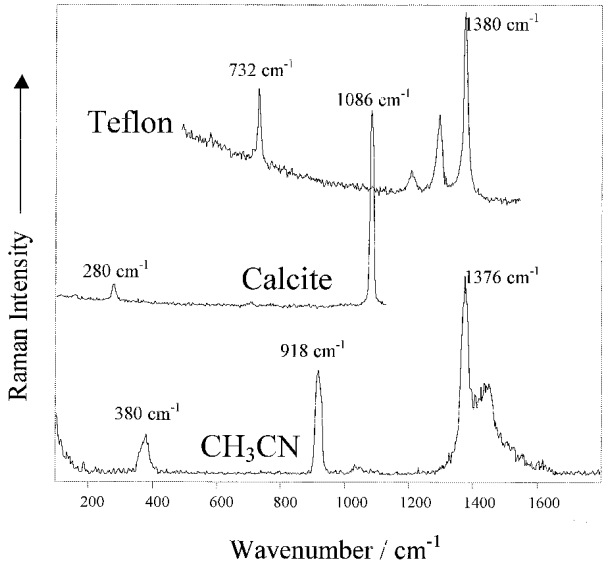

FIG. 4. The 224.3 nm excited Raman spectra of Teflon® block, calcite, and neat acetonitrile. Teflon® and calcite spectra: power = 0.2 mW. Integration time = 20 s. Acetonitrile spectrum: power = 0.3 mW, integration time = 10 s, resolution = 11 cm^{-1}.

the exciting line. We calibrated the spectrometer wavenumber axis using the well-known frequencies of Teflon® and solvent bands.

Horse Heart Myoglobin Studies. Figures 5 and 6 shows 224.3 and 229 nm excited UV Raman spectra of horse heart Mb at pH 7.1 and 2.1. The samples contain 5% by volume acetonitrile, which served as an internal standard. Acetonitrile was used for these Mb studies be-

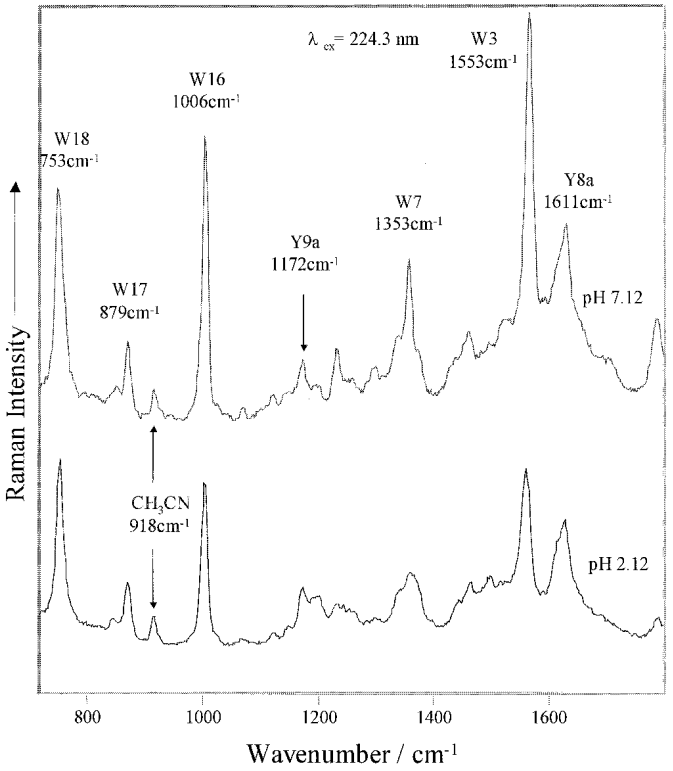

FIG. 5. The 224.3 nm UV Raman spectra of horse heart myoglobin at pH 7.1 and pH 2.1. Spectra have been normalized to the 918 cm^{-1} CH_3CN band intensity. Power = 0.5 mW, integration time = 60 s, resolution = 11 cm^{-1}.

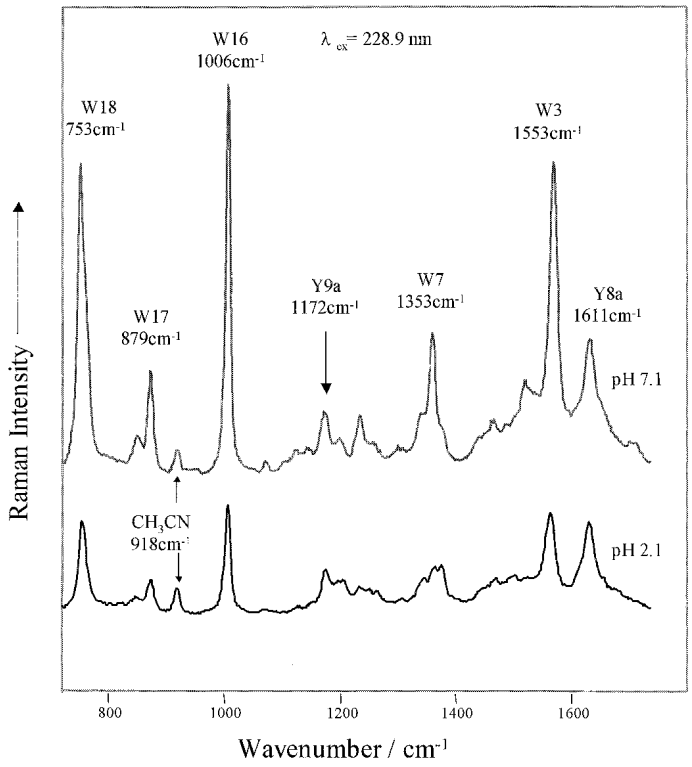

FIG. 6. The 228.9 nm UV Raman spectra of horse heart myoglobin at pH 7.1 and pH 2.1. Spectra have been normalized to the 918 cm^{-1} CH_3CN band intensity. Power = 0.5 mW, integration time = 60 s, resolution = 11 cm^{-1}.

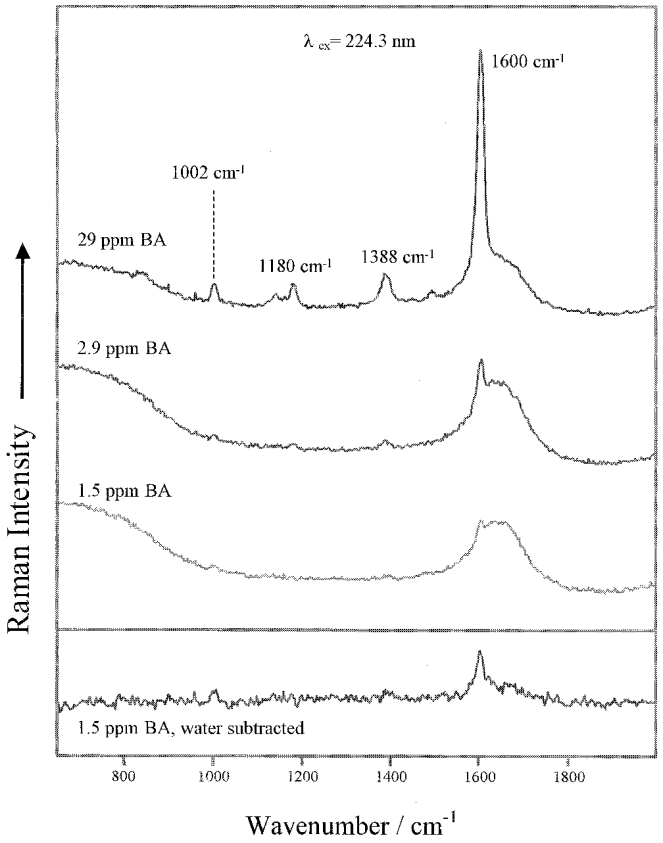

FIG. 7. The 224.3 nm UV resonance Raman spectra of 229 ppm (2.4×10^{-4} M), 2.9 ppm (2.4×10^{-5} M), and 1.5 ppm (1.2×10^{-5} M) dodecyldimethylamine-benzoate solutions. Laser power = 0.5 mW, integration time = 4 min, resolution = 12.5 cm^{-1}. The inset at the bottom shows the solvent-subtracted spectrum of 1.5 ppm dimethyldodecylamine-benzoate solution showing the 1600 cm^{-1} band.

cause the typical internal standards such as perchlorate and sulfate increase the solution ionic strength, which alters the low pH Mb structure. A careful comparison of CD spectra and UVRS in the presence and absence of 5% by volume acetonitrile demonstrates that acetonitrile does not alter the low pH Mb structure.

The 224.3 and 229 nm UVRS are very similar and show Raman bands from only the tyr and trp aromatic amino acids; horse heart Mb has two tyr and two trp.[6] The observed Raman bands result from symmetric in-plane tyr and trp ring vibrations.[17–21] Trp gives rise to the 753 cm^{-1} W18 band, the 879 cm^{-1} W17 band, the 1006 cm^{-1} W16 band, the 1353 cm^{-1} W7 band, and the 1553 cm^{-1} W3 band. Tyr gives rise to the 1172 cm^{-1} $Y9_a$ and the 1611 cm^{-1} $Y8_a$ band. Only the tyr and trp electronic transitions are in resonance at the 224 and 229 nm excitation wavelengths.[17–20] The 918 cm^{-1} band derives from the acetonitrile internal standard.[14]

The 229 nm pH 7.1 Mb spectra are similar to those of Chi et al.[6,21] except that the trp-band relative intensities are increased by ~ 20% compared to those of the tyr. Recent studies in our lab[22] have demonstrated selective bleaching of the Mb trp Raman spectra if the sample flow rate is insufficient to remove photodegraded protein from the illuminated volume.

The 229-trp band Raman cross sections decrease more than threefold as the pH decreases from 7.1 to 2.1. This decrease results from the acid denaturation of the protein, which unfolds the A helix and exposes the attached trp to water. A much smaller decrease occurs for the tyr $Y8_a$ band, because little exposure of the tyr occurs upon the acid denaturation.[6]

The pH 7.1 224.3 nm Mb spectrum appears very similar to that at 229 nm. The major difference is that the W18 and W16 cross sections are decreased by ~ 25%, while the W3 cross section is increased ~ 25% in the 224.3 spectrum compared to the 229 nm spectrum. The $Y8_a$ tyr cross sections are similar. The 224.3 nm pH 2.1 UVRS also shows a ~ threefold decrease in the relative intensities of the trp bands compared to that at pH 7.1. Thus, 224.3 nm excitation can be used to monitor trp and tyr environments in proteins and peptides.

Trace Studies of Aromatic Species. Previous UVRS studies of polycyclic aromatic hydrocarbons demonstrated low ppt detection limits for these species.[3] Figure 7 shows the dependence of the UVRS on the concentration of 1-1 stoichiometric solutions of dodecyldimethylamine and benzoic acid (BA). The dodecyldimethylamine has no resonance transitions until deeper in the UV and, thus, shows no resonance Raman enhanced bands. BA has a strong absorption around 224 nm and thus shows strong resonance enhancement. At 29 ppm (0.24 mM) concentrations the UVRS spectra are dominated by the symmetric, in-plane BA ring vibrations. The only other band observed comes from the broad OH bending vibration of water at ~ 1650 cm^{-1}. The intensities of the BA bands at 1002, 1180, and 1388 cm^{-1} decrease as the BA concentration decreases. Figure 8 shows that the 224.3 nm UVRS intensities of BA increase over the range of 1–300 ppm. The calibration curve is not linear

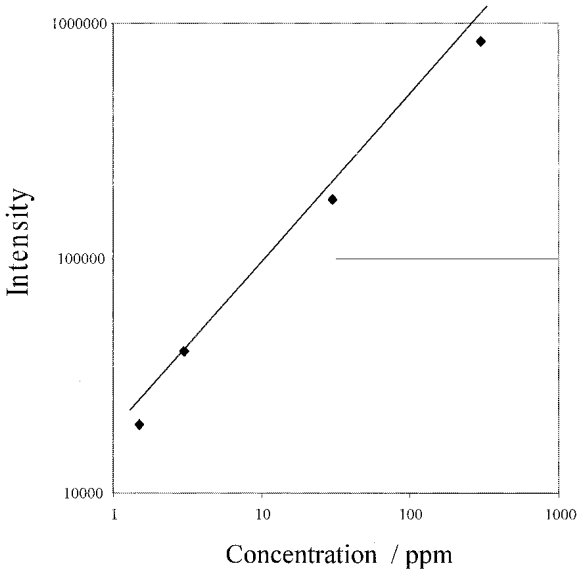

FIG. 8. Dependence of the 1600 cm^{-1} band intensity on BA concentration.

and has a slope less than 1, presumably due to the decreased resonance Raman intensities due to the increased self absorption at the higher analyte concentrations.

The 1600 cm^{-1} BA band is still visible at a concentration of 1.5 ppm. This band is more easily observed if we subtract the water spectrum (Fig. 7). Given the displayed signal-to-noise ratios for the 4 min spectral accumulation times used, we estimate that we have a detection limit of ~ 100 ppb (~ 1×10^{-6} M) by using the ~ 1600 cm^{-1} BA band for detection. Longer accumulation times would give rise to lower detection limits.

CONCLUSION

The new HeAg hollow cathode laser provides an economical and convenient excitation source for UVRS. We have constructed an optimized, inexpensive, simple UV Raman spectrometer for use with this laser source. This 224.3 nm HeAg laser excitation is especially useful for studing the trp and tyr environments in proteins and peptides. It is also useful for detection of aromatic molecules in dilute solutions.

ACKNOWLEDGMENT

We are pleased to acknowledge financial support from NIH Grant 2 R01 GM30741 and Bechtel Bettis Inc.

1. S. A. Asher, Anal. Chem. **65,** 59A, 201A (1993).
2. C. H. Munro, Z. Chi, and S. A. Asher, Laser Focus World **33,** 99 (1997).
3. S. A. Asher, Anal. Chem. **56,** 720 (1984).
4. Z. Chi, X. G. Chen, J. S. W. Holtz, and S. A. Asher, Biochemistry **37,** 2854 (1998).
5. J. S. W. Holtz, J. H. Holtz, Z. Chi, and S. A. Asher, Biophys. J. **76,** 3227 (1999).
6. Z. Chi and S. A. Asher, Biochemistry **37,** 2865 (1998).
7. I. K. Lednev, A. S. Karnoup, M. C. Sparrow, and S. A. Asher, J. Am. Chem. Soc. **121,** 8074 (1999).
8. S. A. Asher, R. W. Bormett, X. G. Chen, D. H. Lemmon, N. Cho, P. Peterson, M. Arrigoni, L. Spinelli, and J. Cannon, Appl. Spectrosc. **47,** 628 (1993).
9. J. S. W. Holtz, R. W. Bormett, Z. Chi, N. Cho, X. G. Chen, V. Pajcini, L. Spinelli, P. Owen, M. Arrigoni, and S. A. Asher, Appl. Spectrosc. **50,** 1459 (1996).
10. S. A. Asher, C. R. Johnson, and J. Murtaugh, Rev. Sci. Instr. **54,** 1657 (1983).
11. B. S. Hudson, P. B. Kelley, L. D. Ziegler, R. A. Desiderio, D. P. Gerrity, W. Hess and R. Bates, *Advances in Lower Spectroscopy,* B. A. Garetz and J. R. Lombardi, Eds. (Wiley, New York, NY, 1986).
12. J. Teraoka, P. A. Harmon, and S. A. Asher, J. Am. Chem. Soc. **112,** 2892 (1990).
13. M. Jones, V. L. DeVito, P. A. Harmon, and S. A. Asher, Appl. Spectrosc. **41,** 1268 (1987).
14. J. M. Dudik, C. R. Johnson, and S. A. Asher, J. Chem. Phys. **82,** 1732 (1985).
15. V. Pajcini, C. H. Munro, R. W. Bormett, R. E. Witkowski, and S. A. Asher, Appl. Spectrosc. **51,** 81 (1997).
16. D. C. Gerstenberger, R. Solanki, and G. J. Collins, IEEE J. Quantum Phys. **16,** 820 (1980).
17. M. Ludwig, C. R. Johnson, and S. A. Asher, J. Am. Chem. Soc. **108,** 3186 (1986).
18. M. Ludwig and S. A. Asher, J. Am. Chem. Soc. **110,** 1005 (1988).
19. J. A. Sweeney and S. A. Asher, J. Phys. Chem. **94,** 4784 (1990).
20. Z. Chi and S. A. Asher, J. Phys. Chem. B.**102,** 9595 (1998).
21. Z. Chi and S. A. Asher, Biochemistry **38,** 9186 (1999).
22. M. C. Sparrow and S. A. Asher, unpublished research.